Nanoscale

Accepted Manuscript

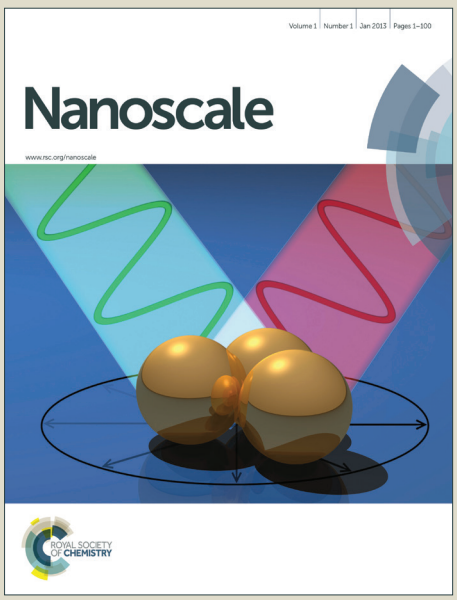

ROYAL SOCIETY OF CHEMISTRY

www.rsc.org/nanoscale

Direct writing of tunable multi-wavelength polymer lasers on a flexible substrate

Tianrui Zhai[*,1], Yonglu Wang[1], Li Chen[2], and Xinping Zhang[*,1]
[1]*Institute of Information Photonics Technology and College of Applied Sciences, Beijing University of Technology, Beijing 100124, China*
[2]*Department of Mathematics & Physics, North China Electric Power University, Hebei 071000, China*
**E-mail: trzhai@bjut.edu.cn and zhangxinping@bjut.edu.cn*

Abstract

Tunable multi-wavelength polymer lasers based on two-dimensional distributed feedback structures are fabricated on a transparent flexible substrate using interference ablation. A scalene triangular lattice structure was designed to support stable tri-wavelength lasing emission and was achieved through multiple exposure processes. Three wavelengths were controlled by three periods of the compound cavity. Mode competition among different cavity modes was observed by changing the pump fluence. Both a redshift and blueshift of the laser wavelength could be achieved by bending the soft substrate. These results not only provide insight into the physical mechanisms behind co-cavity polymer lasers but also introduce new laser sources and laser designs for white light lasers.

Keywords: Tunable polymer lasers, flexible substrates, direct writing.

Many efforts have been made to explore the properties of polymer lasers with particular attention to the electrically pumped organic lasers.[1-7] It offers additional possibilities to realize cheap and versatile light sources. The distributed feedback (DFB) cavities have been investigated extensively because they are the most promising solution for polymer lasers.[1,8-15] Solid-state polymer lasers based on DFB configurations possess a low threshold emission because of their good mode confinement and long gain path.[16,17] Recently, tunable polymer DFB lasers have been successfully fabricated by several groups.[7,18,19] The theory of photonic crystals are employed to understand the emission behavior of DFB polymer lasers.[20-23] However, multi-wavelength polymer DFB lasers based on flexible compound cavities have not been reported. The fabrication of such a laser will not only provide insight into the physical mechanism of co-cavities and tunability but also introduce multi-wavelength laser sources and laser designs. In our previous work, a simple interference ablation technique was proposed to fabricate DFB cavities at large scale and at low cost,[4] which makes the design of compound cavities more effective and convenient.

In this paper, the construction of a tunable polymer DFB laser with compound cavities on a transparent flexible substrate using the laser interference ablation technique is reported. Stable tri-wavelength lasing emission was observed, which could be tuned by bending the soft substrate. The lasing behavior can be explained by the grating diffraction theory due to that the compound cavity is a combination of conventional one-dimensional DFB lasers. The compactness and simplicity of this

laser configuration, combined with its excellent emission properties, enables the development of new laser sources and laser designs.

A typical light-emitting conjugated polymer, poly[(9,9-dioctylfluorenyl-2,7-diyl)-alt-co-(1,4-benzo-{2,1',3}-thiadiazole)] (F8BT) was dissolved in xylene at a concentration of 20 mg/ml before being spin-coated onto a polyethylene terephthalate (PET) film at a speed of 2000 rpm. The PET film (20 mm×20 mm×0.4 mm) was employed as the flexible substrate. The polymer layer on the PET film acts as both an active material and as a "recording" material. The thickness of the polymer layer was about 120 nm. DFB cavities can be constructed on a polymer film using an interference ablation technique as shown in Fig. 1(a). The polymer film was exposed to an interference pattern of two ultraviolet (UV) laser pulses, which was generated by a 355 nm pulsed laser with 5 ns pulse duration, 60 mJ pulse energy, and 1 Hz repetition rate. Ablation of the polymer film occurs at the bright fringes, whereas almost no ablation takes place within the dark fringes. Thus, a DFB cavity corresponding to the interference pattern was realized on the polymer film. The period of the DFB cavity is decided by $\Lambda = \lambda / 2\sin\theta$, which can be adjusted by changing the included angle (θ) between the two laser beams. The spectroscopic properties of the F8BT film before and after UV exposures are illustrated in Fig. S1 in the supporting information, indicating the transient exposure of the polymer film to a 5-ns UV laser pulse did not lead to the degradation of the remaining polymer.

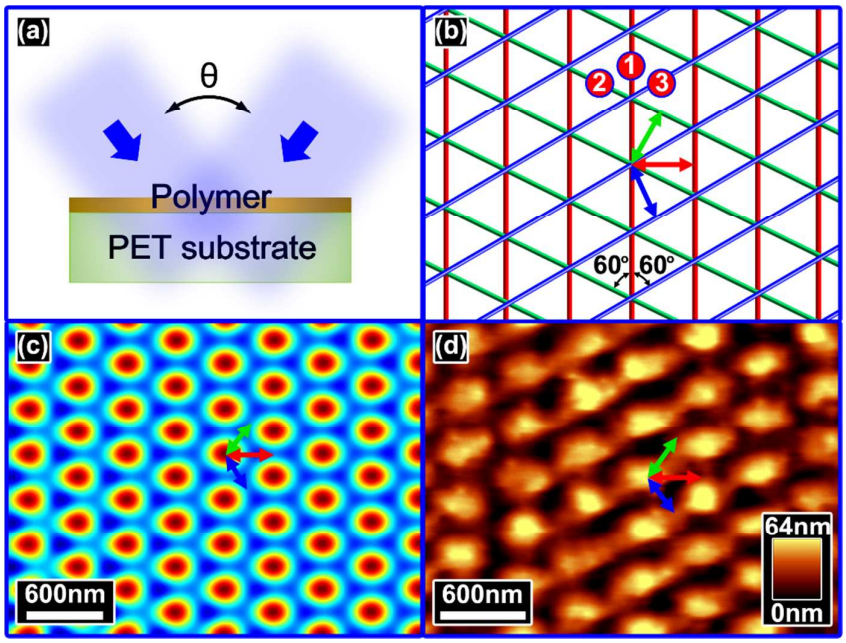

Figure 1. (a) Optical layout of the interference ablation. The period of the interference fringes can be tuned by the included angle θ. (b) A scalene triangular lattice consists of three gratings with different periods, forming by three exposures as identified by ①, ② and ③. The angle between two gratings is 60 degrees. (c) The results of the simulation of a scalene triangular lattice. The maximum and minimum values of the intensity distribution of the interference are indicated by red and blue colors, respectively. (d) AFM image of the scalene triangular lattice structure. The modulation depth is 64 nm. Three periods of the structure were 355 nm, 360 nm, and 365 nm, which are indicated by the blue, green, and red arrows, respectively.

For the fabrication of a scalene triangular lattice structure, three exposures were performed by rotating the sample twice by 60 degrees. Three exposures formed three corrugations with different periods as shown in Fig. 1(b). The results of the simulation of the intensity distribution of the three exposures are demonstrated in Fig. 1(c). The same triangular lattice was fabricated in the polymer materials. After recording the pattern in the polymer layer using interference ablation, the scalene triangular lattice structure could be constructed, which has an effective area with a diameter of about 4

mm. The atomic force microscopy (AFM) image is shown in Fig. 1(d). The three periods of the scalene triangular lattice were 355 nm, 360 nm, and 365 nm, which are indicated by the blue, green, and red arrows, respectively. Note that the modulation depth of the pattern is about 64 nm in the polymer film, which is enough to guarantee the feedback.

For a given period Λ_i of the scalene triangular lattice structure, there are wavelengths λ_i satisfying the Bragg condition,[1]

$$2n_{eff}\Lambda_i = m\lambda_i \quad (i=1, 2, 3)$$

where n_{eff} is the effective refractive index of the structure and m is the order of the diffraction. Thus, the scalene triangular lattice structure is a compound cavity consisting of three morphologically independent cavities. In this work, the second-order structures were employed to achieve a surface-emitting DFB laser. The laser wavelength will be redshifted when the period of the cavity is increased and the tuning rate ($\Delta\lambda/\Delta\Lambda$) is approximately 1.[24] So, if the three periods of the scalene triangular lattice are 355 nm (Λ_1), 360 nm (Λ_2), and 365 nm (Λ_3), the wavelength spacing of the tri-wavelength lasing emission will be 5 nm. Clearly, polymer lasers based on single- and double-grating structures follow the same mechanism as shown in Fig. S3.

The sample was excited by a 400 nm femtosecond pump beam, which had a repetition rate of 1 kHz and a pulse length of 200 fs. The optical layout is shown in the upper panel of Fig. 2(e). The pump beam was incident on the sample at an angle of 20° to facilitate the actual test. The spot size of the pump laser on the polymer film

had a radius of about 2 mm. The pump pulse energy was controlled by a variable optical attenuator. The emission was collected by a spectrometer.

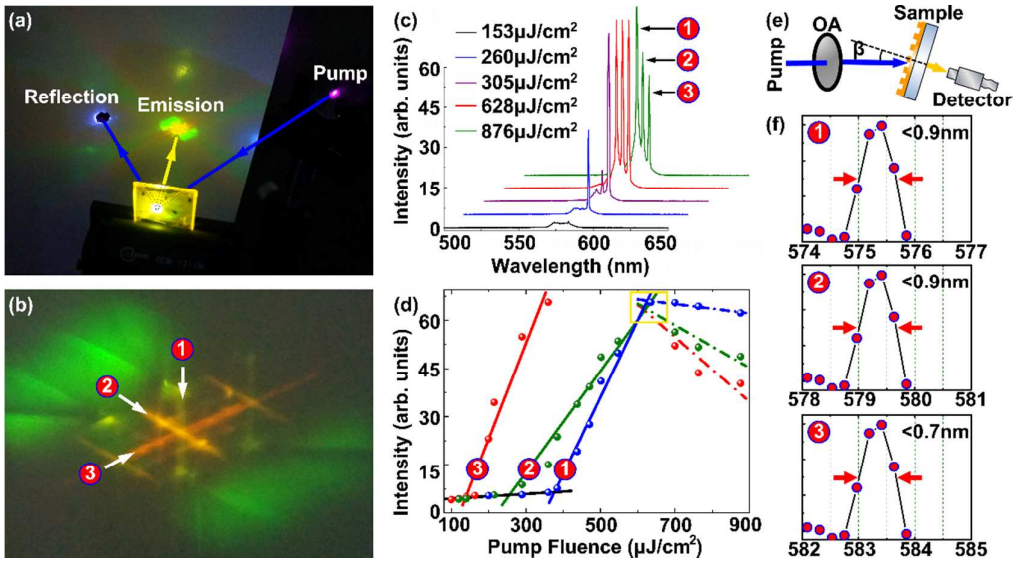

Figure 2. (a) Photograph of the operating tri-wavelength polymer laser. (b) Enlarged view of the laser spot. ①, ②, and ③ identify the emission wavelengths of the 355 nm, 360 nm, and 365 nm cavity, respectively. (c) The measured lasing emission spectra of the tri-wavelength polymer laser at different pump fluences. (d) Output intensity of the polymer laser as a function of the pump fluence, showing that each cavity of the compound cavity has two thresholds. The optimum operating zone is indicated by a yellow square. (e) Optical layout for the experimental measurement. β=20°. (f) The bandwidths (FWHM) of the three emission peaks just above the first threshold.

Figure 2(a) and (b) show a photograph of the lasing device when the pump energy was above the emission threshold. The shape of the laser spot looks like an “asterisk” consisting of three bright lines, which is defined by the Bragg diffraction of the DFB cavity. Multiple laser-emission spots can be observed in Fig. 2(b), which are ascribed to the reflection of the polymer/PET interface. The spectroscopic characterization of the output of the laser device is shown in Fig. 2(c) and (d), where Fig. 2(c) shows the

spectrum of the laser emission at different pump fluences and Fig. 2(d) summarizes the emission intensity as a function of the pump fluence. A stable tri-wavelength lasing emission with approximately 5 nm spacing was observed. The emission wavelengths of the 355 nm, 360 nm, and 365 nm cavities are 575 nm, 579 nm, and 584 nm, respectively. The bandwidths of three peaks just above the threshold are less than 1 nm at full width at half maximum (FWHM) as shown in Fig. 2(f). The emission spectra were recorded as a function of the pump power. An intriguing mode competition occurred, as shown in Fig. 2(b). Each cavity had two thresholds. One threshold was the emergence of the laser emission and the other was the weakening of the laser power. The first threshold of the 355 nm, 360 nm, and 365 nm cavity were 375 $\mu J/cm^2$, 256 $\mu J/cm^2$, and 140 $\mu J/cm^2$, respectively, as shown in Fig. 2(d). The polymer lasers fabricated by interference ablation have similar pump thresholds and narrower emission linewidths with respect to their counterparts fabricated using the conventional technique as shown in Fig. S2, which confirms that the degradation of the polymer film is negligible. The second threshold of the 355 nm, 360 nm, and 365 nm cavity were 625 $\mu J/cm^2$, 624 $\mu J/cm^2$, and 408 $\mu J/cm^2$, respectively, which is attributed to the mode competition. The dominant mode in the compound cavity depletes the exciton, leading to the weakening of the laser power of other cavity modes. The pump slope efficiency of the 355 nm, 360 nm, and 365 nm cavities are measured about 5%, 3%, and 6%, respectively. Thus, the polymer laser based on compound cavities has an optimum operating zone, guaranteeing that the emission intensities of all wavelengths are approximately equal. For the sample shown in Fig.

2(a), the optimum operating zone is indicated by a yellow square in Fig. 2(d), where the pump fluence is around 625 μJ/cm^2. The red curve in Fig. 2(c) demonstrates the emission spectrum of the device operating at the optimum operating zone. The Ocean Optics Maya 2000 PRO spectrometer is employed to characterize the spectra of the laser emission.

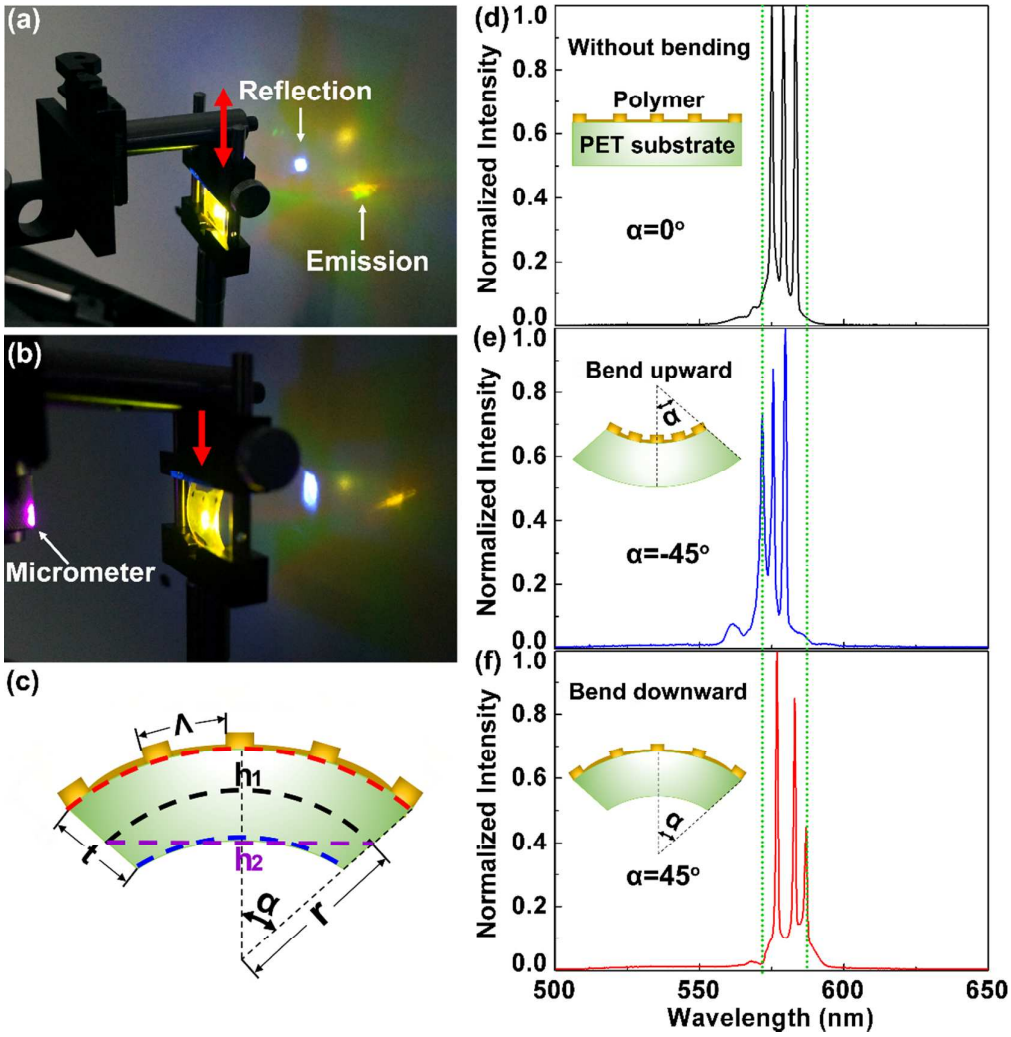

Figure 3. Photographs of the operating laser (a) before and (b) after bending using a sample holder with a height that could be adjusted, as indicated by the red arrow. (c) The influence of the curvature of the substrate on the periodicity of the corrugation. The black dotted line h_1 and the purple dotted line h_2 are the length of the PET film before and after bending, respectively. Λ

is the period of the corrugation, t is the thickness of the PET film, r is the bending radius, and α is half of the bending angle. The red and blue dotted lines denote the two surface lengths of the bent sample. Measured spectra of the polymer laser (d) without bending, (e) with bending upward, and (f) with bending downward, where h_1=20 mm, h_2=18 mm and t=400 μm.

Note that the periodicity of the scalene triangular lattice structure can be altered by taking advantage of the natural flexibility of PET film, which in turn tunes the emission wavelength of the laser device. Upon mechanical bending the emission wavelength shifts toward either the short or long wavelength direction as shown in Fig. 3(d)-(f). During the tuning measurement, the direction of laser emission will change slightly due to the bending curvature of the substrate. In order to ensure the reliability of the experiment, the spatial relative position of the spectrometer and the sample keeps unchanged. Thus, the spectrometer may cannot collect the total energy of the tri-wavelength lasing emission. In addition, when the soft substrate is bent, the laser device deviates from the optimum resonance condition. The laser output power decreases with the bending curvature of the substrate due to the destruction of resonance condition. Thus, the relative power among wavelengths in Fig. 3(d)-(f) suffers a great change.

The flexible laser device was clamped on a sample holder that could have the height adjusted to a precision of 100 μm, as indicated by the red arrow in Fig. 3(a). The operating laser can be quantitatively tuned by gradually bending the laser sample. The curvature of the laser sample was determined by the decrease in height of the sample holder [h_1-h_2 in Fig. 3(c)]. Figure 3(c) illustrates the influence of curvature of the substrate on the periodicity of the corrugation. The surface length of the substrate

changed during the bending process. The outside surface was stretched and the internal surface was compressed, which is denoted by the red and blue dotted lines in Fig. 3(c). The variation in surface length was redistributed to all periods of the corrugation. Thus, the variation of the period of the corrugation on the bent substrate can be estimated using $\Lambda t\alpha/h_1$. For the case in Fig. 3(e) and (f), with h_1=20 mm, h_2=18 mm, t=400 μm, and Λ=360 nm, the variation of the period of the corrugation was around 5 nm, which is in good agreement with the experimental results. To check the repeatability of the device, a bending and restoring experiment is performed. A lens is set before the spectrometer to collect the lasing spectra of the bent sample. Figure 4 demonstrates spectroscopic response of the flexible multi-wavelength polymer lasers. For specific bending direction, one wavelength can keep unchanged while the other two wavelengths are tuned as shown in Fig. S4.

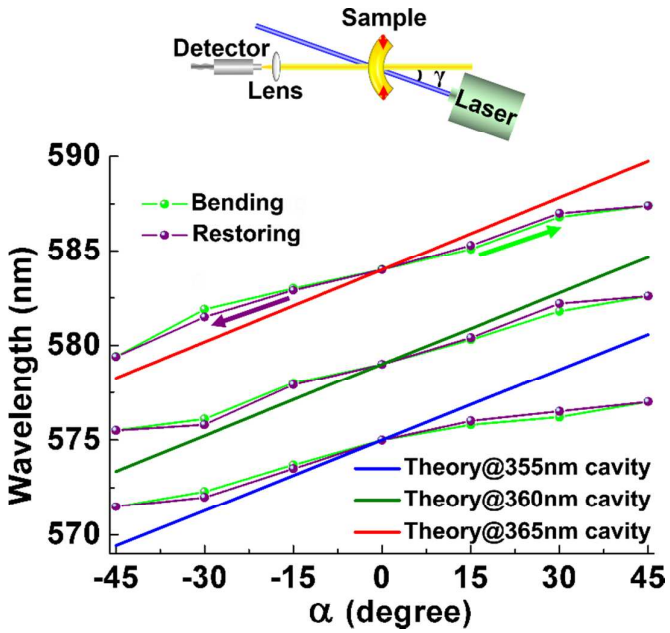

Figure 4. The spectroscopic response of the flexible laser device for bending and restoring processes, respectively. The variation of the laser emission wavelength is calculated by $\Lambda t\alpha/h_1$,

where h_1=20 mm, and t=400 μm. The upper panel shows the measuring setup. The red arrows indicates the stress direction. γ=20°.

In summary, we demonstrated a mechanically tunable tri-wavelength DFB polymer laser based on a scalene triangular lattice cavity fabricated using interference ablation. A stable tri-wavelength output with 0.9 nm linewidth was achieved. Two thresholds were observed with each laser emission because of the mode competition of the co-cavity. This work not only demonstrates a simple and efficient method for fabricating a tunable multi-wavelength DFB polymer laser but also explores the physical mechanisms behind co-cavity polymer lasers.

Acknowledgments The authors gratefully acknowledge the financial support of the National Natural Science Foundation of China (11474014 and 11274031), the Beijing Natural Science Foundation (1132004), and the Beijing Nova Program (2012009).

References

[1] I. Samuel, G. Turnbull, "Organic semiconductor lasers," *Chem. Rev.* **107**, 1272-1295 (2007).

[2] N. Tessler, G. Denton, and R. Friend, "Lasing from conjugated-polymer microcavities," *Nature* **382**, 695-697 (1996).

[3] S. Furumi, "Recent advances in polymer colloidal crystal lasers," *Nanoscale* **4**, 5564-5571 (2012).

[4] T. Zhai, X. Zhang, Z. Pang, and F. Dou, "Direct writing of polymer lasers using interference ablation," *Adv. Mater.* **23**, 1860-1864 (2011).

[5] C. Ge, M. Lu, Y. Tan, and B. T. Cunningham, "Enhancement of pump efficiency of a visible wavelength organic distributed feedback laser by

resonant optical pumping," *Opt. Express* **19**, 5086-5092 (2011).

[6] G. Tsiminis, Y. Wang, A. L. Kanibolotsky, A. R. Inigo, P. J. Skabara, I. D. Samuel, and G. A. Turnbull, "Nanoimprinted organic semiconductor laser pumped by a light-emitting diode," *Adv. Mater.* **25**, 2826-2830 (2013).

[7] S. Döring, M. Kollosche, T. Rabe, J. Stumpe, and G. Kofod, "Electrically tunable polymer DFB laser," *Adv. Mater.* **23**, 4265-4269 (2011).

[8] G. Turnbull, P. Andrew, W. L. Barnes, and I. Samuel, "Operating characteristics of a semiconducting polymer laser pumped by a microchip laser," *Appl. Phys. Lett.* **82**, 313-315 (2003).

[9] T. Voss, D. Scheel, and W. Schade, "A microchip-laser-pumped DFB-polymer-dye laser," *Appl. Phys. B* **73**, 105-109 (2001).

[10] T. Zhai, X. Zhang, and Z. Pang, "Polymer laser based on active waveguide grating structures," *Opt. Express* **19**, 6487-6492 (2011).

[11] H. H. Fang, R. Ding, S. Y. Lu, J. Yang, X. L. Zhang, R. Yang, J. Feng, Q. D. Chen, J. F. Song, and H. B. Sun, "Distributed feedback lasers based on thiophene/phenylene co-oligomer single crystals," *Adv. Funct. Mater.* **22**, 33-38 (2012).

[12] X. Liu, S. Klinkhammer, K. Sudau, N. Mechau, C. Vannahme, J. Kaschke, T. Mappes, M. Wegener, and U. Lemmer, "Ink-jet-printed organic semiconductor distributed feedback laser," *Appl. Phys. Express* **5**, 072101 (2012).

[13] Y. Wang, G. Tsiminis, A. L. Kanibolotsky, P. J. Skabara, I. D. Samuel, and G. A. Turnbull, "Nanoimprinted polymer lasers with threshold below 100 W/cm^2 using mixed-order distributed feedback resonators," *Opt. Express* **21**, 14362-14367 (2013).

[14] J. Herrnsdorf, Y. Wang, J. J. McKendry, Z. Gong, D. Massoubre, B. Guilhabert,

G. Tsiminis, G. A. Turnbull, I. D. Samuel, and N. Laurand, "Micro-LED pumped polymer laser: A discussion of future pump sources for organic lasers," *Laser Photonics Rev.* **7**, 1065-1078 (2013).

[15] J. H. Andrews, M. Crescimanno, K. D. Singer, and E. Baer, "Melt-processed polymer multilayer distributed feedback lasers: Progress and prospects," *J. Polym. Sci. Phys.* **52**, 251-271 (2014).

[16] E. Namdas, M. Tong, P. Ledochowitsch, S. Mednick, J. Yuen, D. Moses, and A. Heeger, "Low thresholds in polymer lasers on conductive substrates by distributed feedback nanoimprinting: progress toward electrically pumped plastic lasers," *Adv. Mater.* **21**, 799-802 (2009).

[17] X. Liu, S. Klinkhammer, Z. Wang, T. Wienhold, C. Vannahme, P.-J. Jakobs, A. Bacher, A. Muslija, T. Mappes, and U. Lemmer, "Pump spot size dependent lasing threshold in organic semiconductor DFB lasers fabricated via nanograting transfer," *Opt. Express* **21**, 27697-27706 (2013).

[18] B. Wenger, N. Tétreault, M. E. Well, and R. H. Friend, "Mechanically tunable conjugated polymer distributed feedback lasers," *Appl. Phys. Lett.* **97**, 193303 (2010).

[19] S. Klinkhammer, X. Liu, K. Huska, Y. Shen, S. Vanderheiden, S. Valouch, C. Vannahme, S. Bräse, T. Mappes, and U. Lemmer, "Continuously tunable solution-processed organic semiconductor DFB lasers pumped by laser diode," *Opt. Express* **20**, 6357-6364 (2012).

[20] S. Riechel, C. Kallinger, U. Lemmer, J. Feldmann, A. Gombert, V. Wittwer, and U. Scherf, "A nearly diffraction limited surface emitting conjugated polymer laser utilizing a two-dimensional photonic band structure," *Appl. Phys. Lett.* **77**, 2310-2312 (2000).

[21] M. Notomi, H. Suzuki, and T. Tamamura, "Directional lasing oscillation of two-dimensional organic photonic crystal lasers at several photonic band gaps," *Appl. Phys. Lett.* **78**, 1325-1327 (2001).

[22] K.-S. Hsu, T.-T. Chiu, P.-T. Lee, and M.-H. Shih, "Wavelength tuning by bending a flexible photonic crystal laser," *J. Lightwave Tech.* **31**, 1960-1964 (2013).

[23] C. L. Yu, H. Kim, N. de Leon, I. W. Frank, J. T. Robinson, M. McCutcheon, M. Liu, M. D. Lukin, M. Loncar, and H. Park, "Stretchable photonic crystal cavity with wide frequency tunability," *Nano Lett.* **13**, 248-252 (2012).

[24] T. Zhai, X. Zhang. "Gain-and feedback-channel matching in lasers based on radiative-waveguide gratings," *Appl. Phys. Lett.* **101**, 143507 (2012).